t, Phys.
nar Sci.
20. W. v. Engelhardt et al., Contrib. Mineral. Petrol. 15, 93 (1967).
21. D. Stöffler, Fortschr. Mineral. 51, 256 (1974).
22. Refractive indices reported in literature do not generally list the wavelength of light used for the measurement. Silica phases have small dispersions which lead to variations of <0.005 in the refractive index at typical wavelengths. Our measured values will tend to be somewhat (~0.002) higher than those using the Na 589-nm line.
23. R. J. Hemley, in High Pressure Research in Mineral Physics, M. H. Manghnani and Y. Syono, Eds. (Mineral Physics Series, American Geophysical Union, Washington, DC, 1987), vol. 2, p. 347.
24. M. B. Kruger and R. Jeanloz, Science 249, 647 (1990).
25. L. E. McNeil and M. Grimsditch, Phys. Rev. Lett. 68, 83 (1992).
26. R. R. Winters, G. S. Serghiou, W. S. Hammack, Phys. Rev. B 46, 2792 (1992).
27. Gas-gun experiments were performed by N. A. Hinsey. We thank M. Wall for help with TEM, W. Beiriger for XRD, V. Chin for photodeveloping, and especially M. L. Olsen for help with TEM analyses. All of this work, done at the Lawrence Livermore National Laboratory, was performed under the auspices of the U.S. Department of Energy under contract W-7405-ENG-48.

17 September 1992; accepted 16 December 1992

Microstructural Observations of α-Quartz Amorphization

Kathleen J. Kingma, Charles Meade, Russell J. Hemley, Ho-kwang Mao, David R. Veblen

Solid-state amorphization is a transformation that has been observed in a growing number of materials. Microscopic observations indicate that amorphization of α-quartz begins with formation of crystallographically controlled planar defects and is followed by growth of amorphous silicon dioxide at these defect sites. Similar transformation microstructures are found in quartz upon quasihydrostatic and nonhydrostatic compression in a diamond-anvil cell to 40 gigapascals and from simple comminution. The results suggest that there is a common mechanism for solid-state amorphization of silicates in static and shock high-pressure experiments, meteorite impact, and deformation by tectonic processes. In general, these results are consistent with recently proposed shear instability models of amorphization.

The phases of silica are important for a wide range of problems in materials science, solid-state physics, and geology (*1*). The formation, stability, and physical properties of the amorphous forms in this system are of particular importance because of their technological applications and the role of silica glass as an archetypal noncrystalline material. Besides conventional melt quenching, amorphous silica can be synthesized from α-quartz by several solid-state processes that include the application of static high pressures (*2*, *3*, *4*), comminution (*5*), and shock compression (*6*, *7*, *8*).

There is now great experimental and theoretical interest in the solid-state crystalline-amorphous transitions of silica and a range of other compounds. Much of the work in this area focuses on descriptions of individual pressure-induced transitions and identification of the similarities they have with conventional phase transitions (such as melting and crystalline-crystalline transitions). To date, there have been a large number of experimental observations of amorphization in different materials (*9*). Despite these observations and the theoretical simulations of amorphization [particularly for SiO_2 (*10*)], a detailed characterization of this transformation is still lacking. Such information is crucial to test recent theoretical models of the transition from crystalline to amorphous states (*10*).

To address these issues, one must determine the manner in which the amorphous phase nucleates, the scale of sample heterogeneity during the transition, and the extent of disordering over a broad range of length scales. Only transmission electron microscopy (TEM) can provide such information because it allows simultaneous imaging and diffraction information at the unit-cell level. Despite these advantages, TEM examination of quench products from diamond-anvil cell experiments is complicated because of the difficulty in handling the small samples and the instability of metastable high-pressure phases under the electron beam. Recently, we have developed experimental techniques to allow routine TEM observations of diamond-cell samples, and here we combine these methods with spectroscopic and optical observations to document the amorphization of α-quartz over four orders of magnitude in length scales.

We examined the transformation mechanism between crystalline and amorphous phases by synthesizing samples of coexisting crystalline and noncrystalline SiO_2 over a wide range of stress conditions. In high-pressure experiments, samples of natural quartz were compressed in the diamond cell under quasihydrostatic and nonhydrostatic conditions (*11*). Phase transformations were monitored with in situ micro-Raman techniques (*3*). Samples were then decompressed from maximum pressure of 15 to 40 GPa to quench the high-pressure transformation microstructures. In comminution experiments, natural quartz was initially ground in a mullite mortar and pestle. After sieving, we ground grains <43 μm (325 mesh) in a ball-milling machine (*12*). The recovered samples from all experiments were characterized by Raman spectroscopy and by optical and electron microscopy (*13*).

TEM images and electron-diffraction patterns showed complete amorphization with no sign of residual crystallinity for diamond-cell samples that were recovered from the highest pressures (>30 GPa). This observation confirms that the loss of sharp diffraction and Raman spectra in previous high-pressure studies (*2*, *3*) was due to amorphization; it was not the result of crystallite size reduction of the parent quartz. In samples that have been either ground or quenched from between 15 and 30 GPa (Fig. 1), the amorphous phase formed in the parent crystalline structure with a characteristic lamellar habit, growing at planar defect sites. As these lamellae grew in size, they maintained subplanar contacts with the crystal, having the same orientation as the original defect. Compared to that of the ground samples, the density of planar features (planar defects and amorphous lamellae) was higher in samples that were quenched from polycrystalline diamond-cell experiments and appeared to rise with increasing maximum pressure. However, detailed examination of a large number of grains from a series of different experiments indicates that the microstructures that were formed by grinding and by static compression are indistinguishable by TEM. The lack of high-temperature effects (such as recrystallization, flow texture, and diffuse boundaries) indicates that the glass lamellae were formed from a solid state transformation; they are not melt-quenched features. In all samples, the planar defects and amorphous lamellae were parallel to rational crystallographic planes. To date, we have found planar features in {001}, {100}, {101}, {0$\bar{1}$1}, {102}, {20$\bar{1}$},

K. J. Kingma, Geophysical Laboratory and Center for High Pressure Research, Carnegie Institution of Washington, Washington, DC 20015, and Department of Earth and Planetary Sciences, The Johns Hopkins University, Baltimore, MD 21218.
C. Meade, R. J. Hemley, H.-k. Mao, Geophysical Laboratory and Center for High Pressure Research, Carnegie Institution of Washington, Washington, DC 20015.
D. R. Veblen, Department of Earth and Planetary Sciences, The Johns Hopkins University, Baltimore, MD 21218.

and {1T1} orientations (*14*).

To monitor optically the growth of the amorphous lamellae, we compressed polished single crystals of quartz quasihydrostatically. For one of these experiments (Fig. 2), initial TEM of an ion-milled foil from the same uncompressed crystal showed no planar defects and hence no preexisting sites for the nucleation of the amorphous phase. In situ optical observations revealed the sudden formation of a set of parallel birefringent planes (Fig. 2A) above 20 GPa. At these pressures, there was also a change in the vibrational modes (Fig. 3), and with further compression, broad bands appeared in the Raman spectra, which indicate a noncrystalline phase (*15*). Optical examination of the decompressed sample (Fig. 2, B to D) shows that the bulk of the crystal is amorphous, whereas the micron-scale planar features are crystalline. Our observations demonstrate that the quenched microstructures in Fig. 2 are not artifacts that were formed upon release of the pressures or shear stresses in these experiments. There is evidence for similar alternating crystalline and noncrystalline bands in anorthite ($CaAl_2Si_2O_8$) that was compressed to 22 GPa (*16*). The microstructures observed directly by optical and TEM methods in our study may be common to crystalline-amorphous transitions in a wide range of silicates.

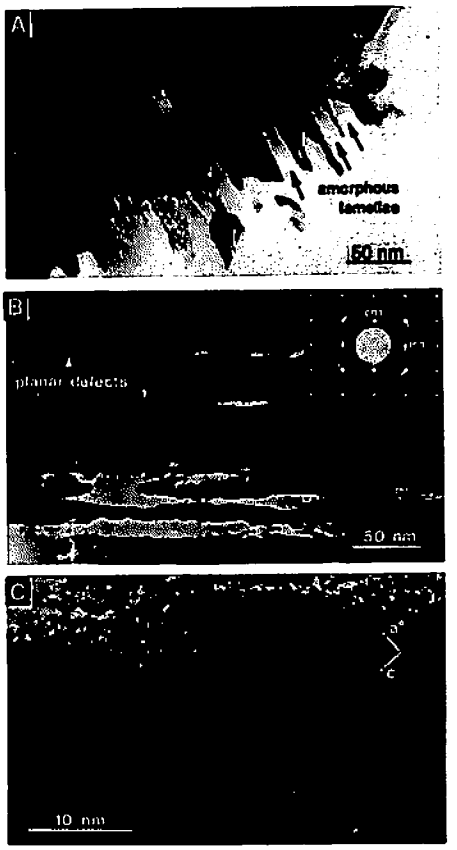

Fig. 1. Representative TEM micrographs that show stress-induced microstructure in quartz samples. All observed microstructures can be divided into two main types: planar defects, which are bounded on either side by quartz, and amorphous lamellae, which range in thickness from 1 to 100 nm. (**A**) Central-beam image (bright-field) showing amorphous lamellae (light bands, three indicated) and crystalline material (dark areas) formed by compression to between 21 and 25 GPa without medium. Electron-beam damage is evident at the thin edge of the grain (widening of lamellae at bottom of micrograph). (**B**) Multiple-beam image from the same compression experiment that shows nucleation and growth of amorphous lamellae (light areas) on planar defects. (**Inset**) Streaking and multiple spots observed in the selected-area electron-diffraction pattern. (**C**) High-resolution micrograph of an amorphous lamella formed during comminution.

Ranging from macroscopic to interatomic length scales, our results provide a basis for a more complete understanding of amorphization and related transitions in quartz. The onset of amorphization, namely the formation of planar defects and the growth of the amorphous phase, has been observed by TEM in both ground and statically compressed samples and is best illustrated in Fig. 1B. Because the proportion of glass is small at this early stage in the amorphization transformation, its signal is overwhelmed by that of quartz in the Raman spectra (Fig. 3). With further compression, the intensity of the Raman bands that are associated with SiO_2 glass increases, which indicates the gradual growth of the amorphous phase. The single crystal in Fig. 2 approaches the end result of the amorphization transition. This grain has transformed almost entirely to a glassy phase, leaving only thin, optically anisotropic plates.

The large differences in the stresses between comminution and static compression experiments indicate that the amorphous state is accessible to quartz over a wide range of pressures and shear stresses (*17*). Whereas static pressures up to 40 GPa were produced in our diamond-cell experiments, the grinding of quartz is limited to differential shear stresses that are comparable to the fracture strength of quartz (*18*). Previous deformation experiments with large shear stresses (1 to 3 GPa) have also produced amorphous silica at pressures and temperatures within the stability field of quartz (*19*). In addition, lamellar diaplectic glass (as well as melt glass) of both optical and TEM scale has been found in shock-compressed SiO_2 from both laboratory (8) and meteorite-impacted samples (*7*, *20*). During shock compression, quartz experiences high transient differential shear stresses, with melting at higher pressures. Finally, deformation bands that contain noncrystalline silicates have been recovered from fault-gouge environments (pseudotachylites) (*21*). In view of the striking similarities between microstructures observed in this study and those produced in a variety of geologic processes, we suggest that such amorphous phases of solid-state origin may be more common in nature than has been thought (*22*, *23*).

Together, our results and previous studies suggest that shear stresses lower the transition pressure between the crystalline and amorphous states of SiO_2. Thus, amorphization probably originates in shearing or

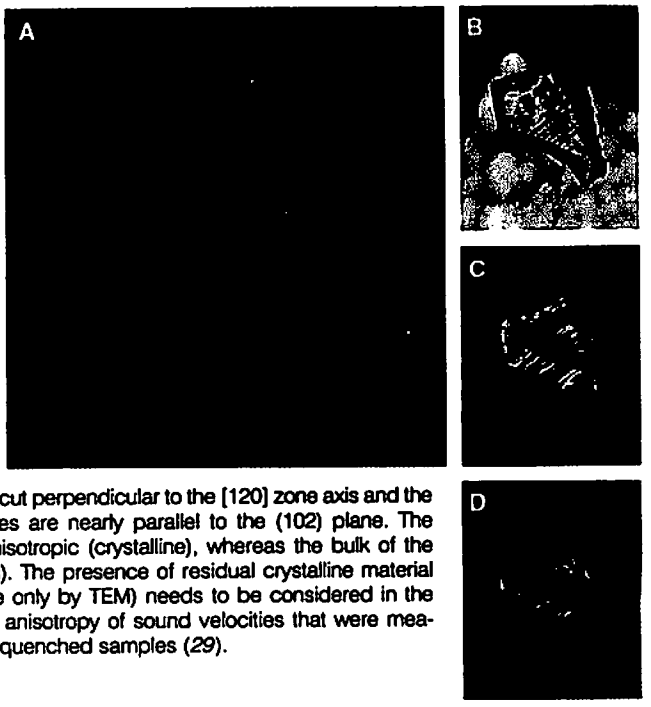

Fig. 2. Optical micrographs of transformed single crystal (**A**) surrounded by neon in the diamond-cell sample chamber at 24.5 GPa and (**B** to **D**) at ambient conditions after recovery from diamond-cell compression. Photographs are taken at 300 K in (A) transmitted white light passing through the diamond anvils, (B) transmitted plane-polarized light, (C) cross-polarized light with some reflected light, and (D) cross-polarized light passing through a 530-nm gypsum plate. The grain, which is approximately 50 by 35 by 15 μm, was cut perpendicular to the [120] zone axis and the pressure-induced planar features are nearly parallel to the (102) plane. The planar features are optically anisotropic (crystalline), whereas the bulk of the sample is isotropic (amorphous). The presence of residual crystalline material such as this (or possibly visible only by TEM) needs to be considered in the interpretation of the anomalous anisotropy of sound velocities that were measured by Brillouin scattering on quenched samples (*29*).

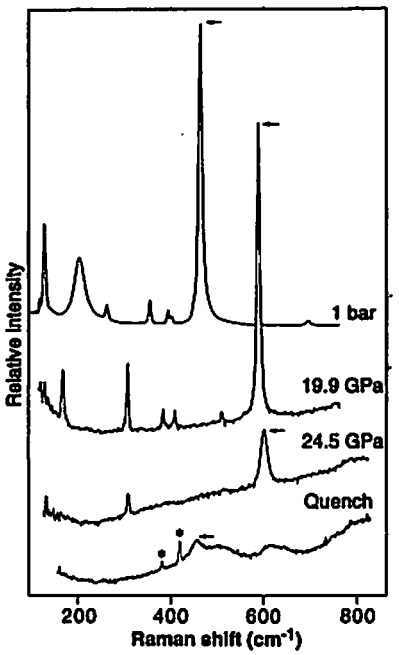

Fig. 3. In situ micro-Raman spectra of the single crystal shown in Fig. 2 with increasing pressure and quenched to ambient conditions. Except for the ruby modes at 379 and 417 cm^{-1} in the quenched spectrum (peaks marked by asterisks), all peaks in the spectra are associated with Raman-active vibrations of SiO_2. Broad bands that appear above 25 GPa confirm the formation of a high-pressure amorphous phase, whereas the persistence of the strongest A_1-symmetry peak (arrows) shows incomplete amorphization through the maximum experimental pressure of 30 GPa. In the spectrum of the quenched sample, the peak at 456 cm^{-1} is from the optically anisotropic residual crystalline phase. The spectra were measured with 514.5-nm excitation by the use of a Dilor (Lille, France) XY spectrograph that was equipped with a charge-coupled device detector.

distortion of the crystal structure. To reconcile the observations of amorphization under disparate stress conditions, we note that quasihydrostatic compression significantly modifies the ambient structure of quartz. As documented in previous x-ray diffraction experiments, there are significant distortions of the SiO_4 tetrahedra and large changes in the angle of Si–O–Si linkages with compression to 15 GPa (*4*). Indeed, there seem to be severe steric constraints to the compression of the polymerized network structure of α-quartz. We have observed a large increase in the density of planar defects with increasing pressure >15 GPa, which indicates that compression-induced lattice distortions produce irreversible strains in quartz at high pressures. Once the amorphous lamellae are formed, we expect that the atomic displacements that are associated with the transformation may produce heterogeneous stresses at the interfaces between the crystalline and amorphous phases. This state of stress probably plays an important role in the growth of the amorphous lamellae (as in Fig. 1) (*24*).

Selected-area electron-diffraction patterns that were obtained across many regions containing amorphous lamellae show streaking and multiple spots (Fig. 1B), which indicate misorientation between the crystalline blocks that are bounded by the lamellae. These effects can be produced by minor angular displacements of blocks across the defects and are consistent with the loss of the single-crystal x-ray diffraction pattern that has been documented with quasihydrostatic compression of quartz to 15 GPa (*4*). However, displacements across defects and lamellae are usually small and may not be evident. For example, close examination of defects shows that lattice fringes are coherent across defect planes. Additionally, scanning electron micrographs show no surface modifications across optical-scale planar features in partially amorphized samples, which would signal intracrystal displacements during the high-pressure transitions.

Our results show that disordering of α-quartz under pressure occurs by multiple processes over vastly different length scales. First, the generation of the amorphous phase results in extensive short-range disordering of SiO_2 within the glassy lamellae. The conversion from a crystalline to an amorphous phase involves bond breaking but with relatively small atomic displacements and without long-range diffusion. In contrast, the misalignment of crystalline blocks across the amorphous lamellae produces disorder over much greater length scales. Thus, the growth and coalescence of amorphous lamellae as pressure increases will produce a continuous change in the length scales of order in the sample. Because of the gradational nature of this transformation, different experimental probes may detect varying amorphization pressures depending on the length scale of the measurement technique (*4*, *25*, *26*). The present results for quartz are closely analogous to the in situ observations of pervasive fracturing that precedes the low-temperature amorphization of H_2O crystalline ice I_h (*27*). Indeed, the results for both materials suggest a close connection between microfracturing, plastic deformation, and amorphization.

Our observations of in situ and quenched transformation microstructures provide important constraints for models of amorphization. For example, the TEM observation of amorphous lamellae in low-pressure comminution experiments indicates that the amorphization process need not be associated with a coordination change. In general, the geometric relationships between the crystalline and amorphous phases are consistent with the presence of a pressure-induced shear instability (*3*, *10*, *22*, *27*). Further, our observations here of crystallographically controlled planar defects show that quartz approaches an intrinsic structural instability limit under a variety of stress conditions. These results show the need to examine defects, crystal-glass interfaces, and grain-boundary stress distributions in theoretical models of the transformation. Solid-state amorphization may have strong parallels to grain-boundary or surface melting phenomena (*28*).

REFERENCES AND NOTES

1. R. B. Sosman, *The Phases of Silica* (Rutgers Univ. Press, New Brunswick, NJ, 1965).
2. R. J. Hemley, A. P. Jephcoat, H. K. Mao, L. C. Ming, M. H. Manghnani, *Nature* 334, 52 (1988).
3. R. J. Hemley, in *High-Pressure Research in Mineral Physics*, M. H. Manghnani and Y. Syono, Eds. (Terra Scientific, Tokyo, and American Geophysical Union, Washington, DC, 1987), pp. 347–359.
4. R. M. Hazen, L. W. Finger, R. J. Hemley, H. K. Mao, *Solid State Commun.* 72, 507 (1989).
5. R. C. Ray, *Proc. R. Soc. London Ser. A* 102, 640 (1923); A. J. Dale, *Trans. Br. Ceram. Soc.* 23, 211 (1923).
6. P. S. De Carli and J. C. Jamieson, *J. Chem. Phys.* 31, 1675 (1959).
7. S. W. Kieffer, P. P. Phakey, J. M. Christie, *Contrib. Mineral. Petrol.* 59, 41 (1976); D. R. Stöffler and U. Hornemann, *Meteoritics* 7, 371 (1972).
8. A. Gratz, *J. Non-Crys. Solids* 67, 543 (1984); J. R. Ashworth and H. Schneider, *Phys. Chem. Miner.* 11, 241 (1985); A. J. Gratz, J. Tyburczy, J. Christie, T. Ahrens, P. Pongratz, *ibid.* 16, 221 (1988); P. F. McMillan, G. H. Wolf, P. Lambert, *ibid.* 19, 71 (1992); A. J. Gratz *et al.*, *ibid.*, p. 267.
9. Pressure-induced amorphization was first documented in H_2O crystalline ice I_h by O. Mishima, L. D. Calvert, E. Whalley [*Nature* 310, 393 (1984)]. Examples of the transformation in other materials are described and reviewed in (*2*); Q. Williams and R. Jeanloz, *Nature* 338, 413 (1989); M. B. Kruger and R. Jeanloz, *Science* 249, 647 (1990); and G. C. Serghiou, R. R. Winters, W. S. Hammack, *Phys. Rev. Lett.* 68, 3311 (1992).
10. S. Tsuneyuki, Y. Matsui, H. Aoki, M. Tsukada, *Nature* 339, 209 (1989); J. R. Chelikowsky, H. E. King, N. Troullier, J. L. Martin, J. Glinneman, *Phys. Rev. Lett.* 65, 3309 (1990); N. Binggeli and J. R. Chelikowsky, *Nature* 353, 344 (1991); J. S. Tse and D. D. Klug, *Phys. Rev. Lett.* 67, 3559 (1991); N. Binggeli and J. R. Chelikowsky, *ibid.* 69, 2220 (1992).
11. All together, ten polycrystalline and five single-crystal samples of α-quartz were compressed at room temperature with Mao-Bell megabar-type diamond-anvil cells, as in (*2*, *3*). Pressures were determined with the ruby-fluorescence method [H. K. Mao, J. Xu, P. M. Bell, *J. Geophys. Res.* 91, 4673 (1986)]. For the quasihydrostatic experiments, both neon, which remains close to a hydrostatic state over the pressure range of this study [P. M. Bell and H. K. Mao, *Carnegie Inst. Washington Yearb.* 80, 404 (1981)] and argon were used as the pressure-transmitting media.
12. The formation of glass upon grinding of quartz was noted in the early experiments in (*5*). See I. J. Lin, S. Nadiv, and D. J. M. Grodzian [*Miner. Sci. Eng.* 7, 313 (1975)] for a review. Despite numerous reports of this phenomenon, there have been no studies of the microstructures that are produced in quartz by grinding.
13. Microscopy was performed at the Johns Hopkins University electron microbeam facilities with a Jeol JXA-8600 Superprobe and a Philips 420 TEM that was equipped with a SuperTwin objective

lens and operated at 120 keV. A video system and a 30-μm condenser aperture were used during TEM examination to minimize beam damage, which can be significant for phases of SiO_2. Crucial to this work was the development of rapid data acquisition techniques to discriminate between amorphous material that was present in the sample and material that was caused by electron-beam damage. Further details that concern experimental techniques will be presented elsewhere [K. J. Kingma *et al.*, in preparation]. An ion mill, operating at 6 kV and accelerating Ar^+ ions from an 18° angle, was used to ion-thin all single-crystal quartz foils.

14. Planar defects and amorphous lamellae are typically observed in only one orientation in individual grains of TEM powder mounts. However, two or more sets of planar features, each in different crystallographic orientations, have been observed in several grains. Because all defects may not be in a diffracting orientation (visible in the TEM), multiple sets within single grains may be the norm. Further statistical analysis of the distribution of orientations is in progress.
15. Detailed examination of the behavior of quartz at these pressures on the basis of in situ x-ray observations will be presented elsewhere [K. J. Kingma, R. J. Hemley, H. K. Mao, in preparation].
16. Q. Williams and R. Jeanloz, in (*9*); an alcohol-water medium was used in this study. Isotropic bands in a decompressed single crystal were observed by optical microscopy.
17. Because the structure of SiO_2 glass changes with pressure [C. Meade, R. J. Hemley, H. K. Mao, *Phys. Rev. Lett.* 69, 1387 (1992)], we expect that the structure of the amorphous phase varies with different synthesis conditions.
18. The fracture strength of quartz at ambient conditions is about 4 GPa [M. S. Paterson, *Experimental Rock Deformation—The Brittle Field* (Springer-Verlag, New York, 1978), p. 30]. However, stress concentrations in localized areas such as fractures and crack tips may be much higher. Amorphous SiO_2 on a TEM scale has been found along fractures that were formed during indentation deformation experiments that tested the fracture toughness of natural quartz [C. C. Ferguson, G. E. Lloyd, R. J. Knipe, *Can. J. Earth Sci.* 24, 544 (1987)]. Stress-induced amorphization has also resulted from room temperature indentation of silicon and germanium single crystals [D. R. Clarke, M. C. Kroll, P. D. Kirchner, R. F. Cook, B. J. Hockey, *Phys. Rev. Lett.* 60, 2156 (1988)] and from mechanical scratching of silicon [K. Minowa and K. Sumino, *ibid.* 69, 320 (1992)].
19. J. M. Christie and A. J. Ardell, *Geology* 2, 405 (1974); L. N. Dell'Angelo, *Eos* 71, 458 (1991).
20. Similarities between amorphous phases that are produced by diamond-cell compression and by shock impact of silicates are described in (*16*). Luminescence associated with extreme localized heating has been observed during shock of quartz single crystals [P. J. Brannon *et al.*, *J. Appl. Phys.* 54, 6374 (1983)]. No such luminescence was observed during our static compression experiments.
21. Examining a large number of samples, H.-R. Wenk [*Geology* 6, 507 (1978)] concluded that pseudotachylites are formed by cataclasis, not by melting. Further examples are reviewed by R. A. Yund, M. L. Blanpied, T. E. Tullis, and J. D. Weeks [*J. Geophys. Res.* 95, 15589 (1990)]. We suggest that solid-state amorphization that is associated with deformation at relatively low temperatures may give rise to these features.
22. C. Meade and R. Jeanloz, *Science* 252, 68 (1991).
23. The high solubility of amorphous phases may obscure their formation in the geologic record. Amorphization of geologic materials may also occur in subduction zone environments (*22*).
24. S. Morris, *Proc. R. Acad. London* 436, 203 (1992); stresses at crystalline-amorphous interfaces may have compressional, shear, or even tensile components. Additionally, even in the presence of a hydrostatic medium the formation of multiple crystalline blocks will produce nonhydrostatic stress at the block interfaces, which will in turn drive the breakdown of the parent crystalline form.
25. C. Meade, R. Jeanloz, R. J. Hemley, in *High Pressure Research: Applications to Earth and Planetary Sciences*, Y. Syono and M. H. Manghnani, Eds. (Terra Scientific, Tokyo, and American Geophysical Union, Washington, DC, 1992), pp. 485–492.
26. It will be important to examine the behavior of quartz at still higher pressures. Additionally, the role of amorphization of a metastable high-pressure phase or phases upon decompression should also be examined [as in (*27*)].
27. R. J. Hemley, L. C. Chen, H. K. Mao, *Nature* 338, 638 (1989).
28. B. Pluis, W. D. van der Gon, J. W. M. Frenken, J. F. van der Veen, *Phys. Rev. Lett.* 59, 2678 (1987).
29. L. E. McNeil and M. Grimsditch, *ibid.* 68, 83 (1992).
30. We thank Q. Williams, R. Jeanloz, A. J. Gratz, R. M. Hazen, and R. E. Cohen for helpful discussions and correspondence. Supported by National Science Foundation (NSF) grants EAR-8920239 and EAR-9117858 (R.J.H. and H.K.M.) and NSF grant EAR-8903630 (D.R.V.).

15 September 1992; accepted 23 December 1992

The Hydrolytic Water Molecule in Trypsin, Revealed by Time-Resolved Laue Crystallography

Paul T. Singer, Arne Smalås, Robert P. Carty, Walter F. Mangel, Robert M. Sweet*

Crystals of bovine trypsin were acylated at the reactive residue, serine 195, to form the transiently stable *p*-guanidinobenzoate. Hydrolysis of this species was triggered in the crystals by a jump in pH. The hydrolysis was monitored by three-dimensional Laue crystallography, resulting in three x-ray diffraction structures, all from the same crystal and each representing approximately 5 seconds of x-ray exposure. The structures were analyzed at a nominal resolution of 1.8 angstroms and were of sufficient quality to reproduce subtle features in the electron-density maps for each of the structures. Comparison of the structures before and after the pH jump reveals that a water molecule has positioned itself to attack the acyl group in the initial step of the hydrolysis of this transient intermediate.

The serine protease trypsin has been studied extensively for decades, but there are still gaps in our understanding of the mechanism of proteolysis by trypsin. Like all serine proteases, trypsin acts in a two-step process. First, nucleophilic attack on a peptide bond by a serine hydroxyl group leads to the breaking of the peptide and formation of an ester bond between the carboxyl group and the serine hydroxyl. The hydroxyl group is activated by a nearby histidine and a buried aspartate, which form the "catalytic triad" (*1*). This intermediate is subsequently hydrolyzed by a water molecule, regenerating the hydroxyl and releasing the second half of the cleaved protein. That this water molecule itself is activated by the catalytic triad, in a mechanism that mirrors the initial reaction, has always been assumed. In order to explore the hydrolysis of the ester intermediate, we have prepared a transiently stable species by reaction of the enzyme with *p*-nitrophenyl guanidinobenzoate to form *p*-guanidinobenzoyl (GB) trypsin (*2*, *3*). The form of the trypsin crystals that results has been investigated independently by Bartunik and co-workers (*4*). Release of the GB group can be controlled by pH; it is stable for days at low pH but only for hours at slightly above neutral pH. We used the Laue method of white-beam crystallography to collect x-ray diffraction data from a crystal of GB trypsin first at low pH, then immediately after the jump to high pH, and 90 min later at the higher pH. We addressed the following questions: Is the 1- to 2-min time resolution provided by the Laue measurement sufficient to trap a meaningful state along the catalytic pathway? Can the Laue method, which provides an inherently poor signal-to-noise ratio for diffraction data, reveal details as small as the motion of a side chain or water molecule? Can this model system provide insight into catalysis by serine proteases in general?

In a preliminary report of this work (*5*), we described the procedures used for the collection of Laue diffraction data. A single crystal of GB-substituted trypsin, measuring 1.0 mm by 0.4 mm by 0.4 mm, was mounted in a flow cell at pH 5.5. Between five and seven x-ray exposures were taken at beamline X26-C of the National Synchrotron Light Source. In order to counter damage of the specimen by the x-ray beam, the exposures were divided between two separated portions of the crystal, the spec-

P. T. Singer, Biology Department, Argonne National Laboratory, Argonne, IL 60439.
A. Smalås, Institute of Mathematical and Physical Science, University of Tromsø, N-9000 Tromsø, Norway.
R. P. Carty, Department of Biochemistry, State University of New York Health Science Center, Brooklyn, NY 11203.
W. F. Mangel and R. M. Sweet, Biology Department, Brookhaven National Laboratory, Upton, NY 11973.
*To whom correspondence should be addressed.